Journal of
PERIODONTAL RESEARCH

J Periodont Res 2011; 46: 118–125

JOURNAL OF PERIODONTAL RESEARCH
doi:10.1111/j.1600-0765.2010.01321.x

Gene-expression profiles of epithelial cells treated with EMD *in vitro*: analysis using complementary DNA arrays

I. Kapferer[1], S. Schmidt[2], R. Gstir[3], G. Durstberger[4], L. A. Huber[3], I. Vietor[3]

[1]Department of Operative Dentistry, Dental School, Innsbruck Medical University, Innsbruck, Austria, [2]Department of Internal Medicine, Division of Hematology and Oncology, Innsbruck Medical University, Innsbruck, Austria, [3]Division of Cell Biology, Biocenter, Innsbruck Medical University, Innsbruck, Austria and [4]Department of Periodontology, Bernhard-Gottlieb Dental School, Vienna Medical University, Vienna, Austria

Kapferer I, Schmidt S, Gstir R, Durstberger G, Huber LA, Vietor I. Gene-expression profiles of epithelial cells treated with EMD in vitro*: analysis using complementary DNA arrays. J Periodont Res 2011; 46: 118–125. © 2010 John Wiley & Sons A/S*

Background and Objective: During surgical periodontal treatment, EMD is topically applied in order to facilitate regeneration of the periodontal ligament, acellular cementum and alveolar bone. Suppresion of epithelial down-growth is essential for successful periodontal regeneration; however, the underlying mechanisms of how EMD influences epithelial wound healing are poorly understood. In the present study, the effects of EMD on gene-expression profiling in an epithelial cell line (HSC-2) model were investigated.

Material and Methods: Gene-expression modifications, determined using a comparative genome-wide expression-profiling strategy, were independently validated by quantitative real-time RT-PCR. Additionally, cell cycle, cell growth and *in vitro* wound-healing assays were conducted.

Results: A set of 43 EMD-regulated genes was defined, which may be responsible for the reduced epithelial down-growth upon EMD application. Gene ontology analysis revealed genes that could be attributed to pathways of locomotion, developmental processes and associated processes such as regulation of cell size and cell growth. Additionally, eight regulated genes have previously been reported to take part in the process of epithelial-to-mesenchymal transition. Several independent experimental assays revealed significant inhibition of cell migration, growth and cell cycle by EMD.

Conclusion: The set of EMD-regulated genes identified in this study offers the opportunity to clarify mechanisms underlying the effects of EMD on epithelial cells. Reduced epithelial repopulation of the dental root upon periodontal surgery may be the consequence of reduced migration and cell growth, as well as epithelial-to-mesenchymal transition.

Ines Kapferer, DMD, MSc, Reichenauerstraße 46, 6020 Innsbruck, Austria
Tel: 0043 512 504 27221
Fax: 0043 512 504 27184
e-mail: ines.kapferer@gmx.net

Key words: enamel proteins; epithelium; microarray; wound healing

Accepted for publication July 19, 2010

Clinical and histological investigations have demonstrated that intrasurgical application of porcine EMD results in the regeneration of various periodontal tissues, such as alveolar bone, acellular cementum and new periodontal ligament (1–4). Wound healing following conventional periodontal therapy frequently does not result in regeneration but rather in the down-growth of a long junctional epithelium (1). When applied to denuded root surfaces, EMD precipitates to form an extracellular matrix layer, potentially supporting interactions with cells in adjacent tissues (4). EMD is produced by Hertwig's epithelial sheath during dentinogenesis and is commercially available from acid extracts of enamel buds of 6-mo-old pigs. The composition is rather heterogeneous and includes concentrated amelogenin components, degradation products and specific splicing products, along with

many unknown molecules (5,6). The complexity of both the composition and the proteolytic activity of EMD underscores the difficulty of ascribing the biological activity to any single component (6). EMD produces differential effects on mesenchymal and epithelial cells; for example, it increases the proliferation of gingival fibroblasts in cell cultures (7,8), but retards epithelial cell proliferation (4,8). It was proposed that the antiproliferative effect of EMD on epithelial cells is responsible for the desirable retarded epithelial down-growth alongside the dental root during the process of periodontal regeneration (8,9). In contrast, many clinicians have observed accelerated epithelial soft-tissue wound healing upon intrasurgical application of EMD (10). The mechanisms of EMD-mediated epithelial down-growth inhibition have not yet been clarified, and studies using epithelial cells are rare.

Here we analyzed the genome-wide expression of epithelial cells following EMD treatment and the effects of EMD on cell migration and cell growth. A set of EMD-regulated genes, which might be responsible for the reduced epithelial down-growth after EMD application, was successfully defined and validated.

Material and methods

Cell culture

The human squamous carcinoma HSC-2 cell line was provided by the Cell Resource Centre for Biomedical Research, Tohoku University (Sendai, Japan). Cells were cultured in Dulbecco's modified Eagle's minimal essential medium (DMEM; AppliChem, Darmstadt, Germany), supplemented with 10% fetal calf serum (FCS) (Gibco, Eggenstein, Germany) and 1% penicillin/streptomycin (Gibco), at 37°C in a 5% CO_2/air atmosphere. The tissue culture medium was changed every 2 d. These transformed cells were chosen as a model for oral epithelial cells because they continue to display a moderately mature epithelial phenotype while at the same time offering experimental advantages. All experiments were performed using cells between passages 6 and 12.

Treatments

Commercial lyophilized EMD was provided by the manufacturer (Straumann, Basel, Switzerland) and dissolved in 0.1% acetic acid (Carl Roth, Karlsruhe, Germany) to yield a stock solution of 10 mg/mL, as recommended by the manufacturer. The stock solution was aliquoted and stored at −80°C. If not stated otherwise, this stock solution was further diluted in cell culture medium to yield a concentration of 100 μg/mL of EMD, which was determined, by preliminary studies (*in vitro* wound-healing and proliferation assays), as the optimal concentration for use in our experiments. In pilot experiments, we firmly excluded any appreciable effects of acetic acid on cell proliferation or on the *in vitro* wound healing of HSC-2 cells, treated from 2 h up to 5 d.

Oligonucleotide microarray analysis

In order to apply a comparative genome-wide expression-profiling strategy, kits from Affymetrix were used for target preparation before hybridization to hgu133 Plus 2.0 microarrays (Affymetrix, Santa Clara, CA, USA). HSC-2 cells were cultured in six-well plates (5×10^4 cells per well) at 37°C for 24 h and subsequently stimulated with 100 μg/mL of EMD for 2, 20 or 120 h. Cells treated for 120 h were split after 72 h. There was one single replicate per time-point. Control cells were treated for 20 or 120 h (split after 72 h) with DMEM containing 10% FCS. Total RNA was extracted.

mRNA was prepared using TriReagent (Molecular Research Center, Cincinnati, OH, USA) and purified by RNeasy (Qiagen, Hilden, Germany) according to the manufacturers' instructions. The quantity and integrity of mRNA was evaluated by calculating the 260/280 nm absorbance ratio and by using Agilent lab-on-a-chip technology (2100 Bioanalyzer; Agilent, Palo Alto, CA, USA). Then, 1.5 μg of high-quality mRNA was processed into a biotinylated hybridization target for microarray analysis, using the corresponding kits from Affymetrix, and hybridized to hgu133 Plus 2.0 microarrays. Fluorescence signal intensities were determined using the Affymetrix GeneChip Scanner 3000 and the GCOS software version 1.2 (Affymetrix), according to the manufacturer's recommendations. Data processing and analysis were performed using Bioconductor packages for the statistical language R (11). Robust multiarray analysis was applied for normalization. Consecutively differentially expressed genes were determined and tested for hyper-represented gene ontology (GO)-terms. A list of 81 probe sets was used for further analysis, as described in the Results section. These 81 probe sets were used for GO-analysis. The GO-analysis was performed for all three categories of this ontology (cellular component, molecular function and biological process). In order to identify common regulatory patterns, hierarchical cluster analysis was applied to the 81 candidate probe sets.

Data verification by real-time RT-PCR

Seventeen probe sets were excluded based on unreliable annotation. The remaining 64 probe sets, corresponding to 43 genes, were selected for data validation by quantitative real-time RT-PCR, using TaqMan® low-density arrays (Applied Biosystems, Foster City, CA, USA). Five genes [glyceraldehyde-3-phosphate dehydrogenase (GAPDH), hypoxanthine phosphoribosyltransferase 1, transferrin receptor, TATA box binding protein, phosphoglycerate kinase 1)] were selected as controls. Total RNA was extracted from HSC-2 cells, treated with 100 μg/mL of EMD for 2, 20 or 120 h and reverse transcribed into complementary DNA (cDNA). These experiments were performed in triplicate. cDNA was assayed by real-time RT-PCR using microfluidic cards (Applied Biosystems assays) and, again, each sample was applied three times. One-hundred nanograms of cDNA was combined with 1× TaqMan® Universal Master Mix (Applied Biosystems) and loaded into each well.

Table 1. Microarray analysis

Duration of treatment with EMD	Regulated genes (*n*)		
	Total	Up-regulated	Down-regulated
2 h	118	69	49
20 h	216	154	62
120 h	430	237	193

EMD was used at 100 μg/mL.

The microfluidic cards were cycled at 50°C for 2 min and 94.5°C for 10 min, followed by 40 cycles at 97°C for 30 s and 59.7°C for 1 min. Data were collected and analysed using the SDS 2.1 software (Applied Biosystems) Table 1.

In vitro wound-healing assay

The effects of EMD on HSC-2 cell migration were analysed using an *in vitro* wound-healing model (12). HSC-2 cells were seeded at a density of 11.5×10^4 cells into each well of a six-well plate and incubated for 24 h at 37°C until confluent. Using a yellow pipette tip, a scratch (1 mm in diameter) was created through the centre of the cell layer. Detached cells were removed by washing three times with phosphate-buffered saline (PBS) and the remaining adherent cells were treated with DMEM containing 2% FCS (negative control), or with DMEM containing 2% FCS and 100 μg/mL of EMD. Lower FCS concentrations were used to minimize cell proliferation and to induce cell migration, as previously described (12). The cells were photographed every 2 h, using an inverted light microscope equipped with a charge coupled device camera. Experiments were performed in triplicate.

Cell growth analysis

The influence of EMD on HSC-2 cell proliferation was determined by the nonradioactive, colorimetric MTT [(3-(4,5-dimethylthiazol-2-yl)-2,5-diphenyltetrazolium bromide] assay (Promega, Madison, WI, USA). HSC-2 cells were seeded at a density of 1×10^4 cells into each well of 96-well plates and incubated at 37°C. After 24 h, the cells were treated with 100 μg/mL of EMD for 2, 20, 72 or 120 h. Cells treated for 120 h were split after 72 h. Control cells for all time-points were treated with DMEM supplemented with 10% FCS. Then, 0.45 mg/mL of MTT was added consecutively to each well and the cells were incubated at 37°C for a further 4 h. At the end of this incubation period, the cells were incubated for a further 2 h with the solubilization reagent (200 μL of dimethyl sulphoxide). The test absorbance at 570 nm and reference absorbance at 630 nm were measured using an ELISA plate reader (Corning Costar, Corning, NY, USA). Experiments were performed in triplicate.

Cell cycle analysis measured by propidium iodide staining

HSC-2 cells were cultured in six-well plates (at a density of 5×10^4 cells per well) at 37°C for 24 h and subsequently stimulated with 100 μg/mL of EMD for 2, 20, 72 or 120 h. Cells treated for 120 h were split after 72 h. Control cells for all time-points were treated with DMEM supplemented with 10% FCS. The cells were harvested by trypsinization and resuspended in 1 mL of DMEM containing 10% FCS. The cell suspensions were washed with 1 mL of PBS, fixed with 2.5 mL of 70% ethanol and incubated on ice for 1 h. The cell pellet was resuspended in 500 μL of propidium iodide solution (Sigma, Deisenhofen, Germany), supplemented with 0.1 mg/mL of RNase A (Fermentas, St Leon-Rot, Germany) and 0.1% Triton X-100 (Sigma), and incubated for 15 min at 37°C. Then, the cells were washed, resuspended in PBS and analyzed in a FACSCalibur flow cytometer (BD Bioscience, Heidelberg, Germany), using the software FLOWJO (Tree Star San Carlos, CA, USA). The experiments were performed in triplicate.

Statistical analysis

GO and GOstats bioconductor packages were used for oligonucleotide microarray analysis. Hypergeometric *p*-values for over-representation of the selected genes were calculated by comparison with all GO terms in the induced GO graph. The association between the regulation values of the microarray and quantitative real-time RT-PCR data was assessed via the generation of regression lines and the calculation of Pearson correlation coefficients for each probe set individually, and for overall data comparison. Differences in cell growth and cell cycle analyses were analyzed using the Student's *t*-test. Probability levels of ≤ 0.05 were considered to indicate statistical significance. Statistical calculation was carried out using VASSARSTATS® VASSAR COLLEGE, Poughkeepsie, NY, USA.

Results

Oligonucleotide microarray analysis

A total of five expression profiles were generated from samples treated with EMD for 2, 20 or 120 h, and from two controls. Differentially expressed genes were detected upon comparison of normalized expression data from EMD-treated cells with that of control cells. Differential expression was based on M-value cut-off selection. Overall, the number of regulated genes was not very high. Therefore, in order not to lose potential candidate genes, we used a lower threshold of $M < -0.7$ or $M > 0.7$, instead of $M > 1$ or $M < -1$, as used in the original analysis. *M*-values of 0.7/−0.7 correspond to 1.6-fold induction/repression. Comparing both of the controls, we found only two genes (interferon-induced protein 44-like and retinoic acid receptor, alpha) that were regulated more than 1.6-fold. A total of 669 probe sets were regulated at least once in the comparisons. However, only 90 of these were regulated at two out of the three time-points. Four genes (NADPH oxidase 4, wingless-type MMTV integration site family, member 5B, protein tyrosine phosphatase,

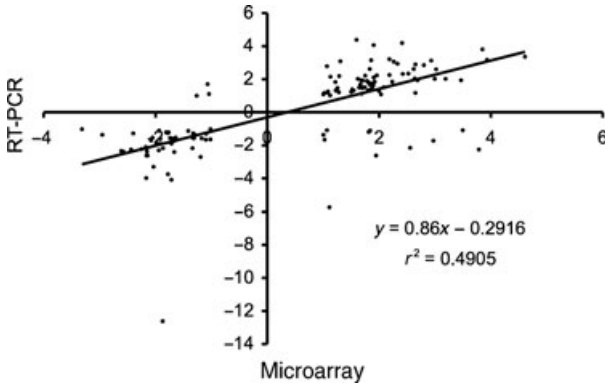

Fig. 1. Regression and correlation. Relationship between the fold-regulation values, obtained by RT-PCR (*y*-axis) and by the Affymetrix microarray (*x*-axis), of 43 commonly regulated genes after 2, 20 or 120 h of treatment of HSC-2 cells with 100 μg/mL of EMD. Pearson correlation coefficient $r = 0.700$. Data sources are provided in Table 3.

receptor type, K, and transmembrane, prostate androgen induced RNA) were up-regulated at all time-points, whereas claudin 1 was down-regulated at all time-points. Selection criteria for candidate probe sets to be reconfirmed using an independent RT-PCR-based technique were: regulation of ≥ 1.6-fold; regulation at two out of the three time-points; and concordant up- or down-regulation. Applying these criteria resulted in a candidate probe set list of 81 probe sets (Table S1).

Data validation by quantitative real-time RT-PCR

Seventeen probe sets were excluded based on unreliable annotation. The remaining 64 probe sets, which correspond to 43 genes, were selected for data validation by real-time RT-PCR using TaqMan® low-density arrays (Applied Biosystems). The expression of 32 regulated genes correlated well with the regulation found in the microarray data, yielding a Pearson correlation coefficient, r, of > 0.6 (Table S1). For the 43 genes assayed, the overall Pearson correlation coefficient was 0.700 for all microarray vs. RT-PCR analyses (Fig. 1).

Hierarchical cluster analysis

In order to delineate a potentially underlying pathway, we determined patterns of co-regulation by hierarchical clustering of the regulation values of the 81 candidate probe sets. Thereby we identified five clusters of genes (Fig. 2), three clusters of up-regulated genes and two clusters of down-regulated genes. Forty-two probe sets were up-regulated in EMD-treated cells at all-time points (2, 20 and 120 h). Among these, two clusters were coregulated genes that showed increasing

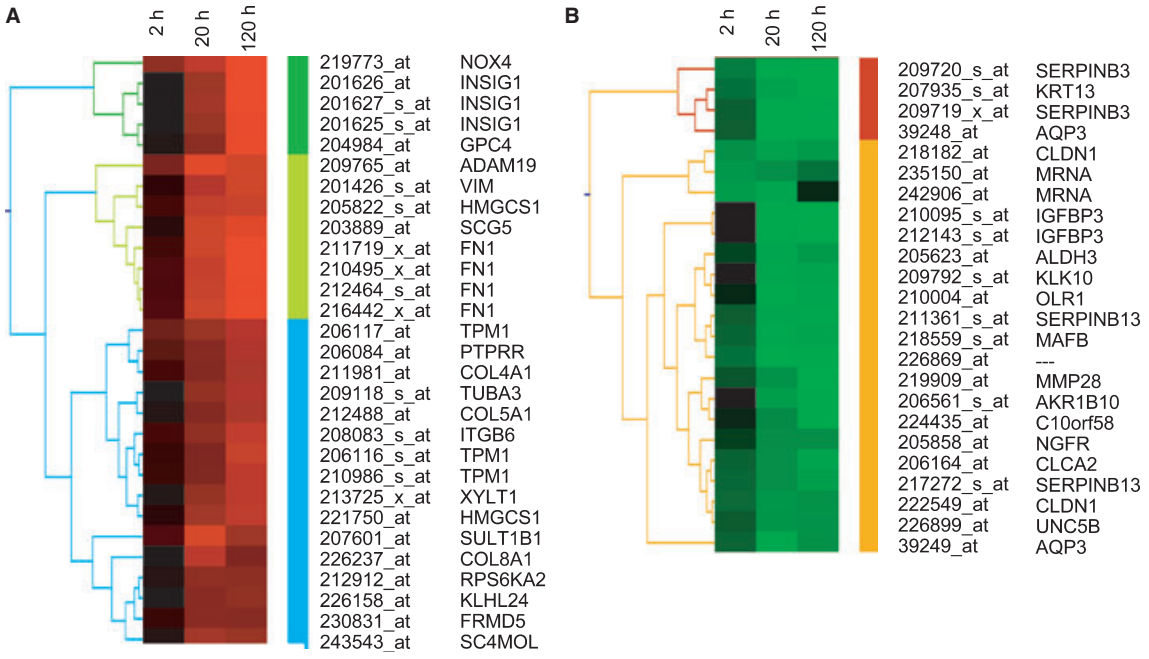

Fig. 2. Hierarchical clustering. The relative expression levels of the genes in HSC-2 cells treated with 100 μg/mL of EMD for 2, 20 or 120 h are shown in dendrograms. By hierarchical clustering, a two-dimensional table of genes (rows) and experiments (columns) was produced in which genes that show a similar pattern of regulation (clustering *M*-values) or a pattern of similar expression (clustering expression values) over the experiments become arranged closely together. (A) Genes that were up-regulated when compared with the control are marked red. Among those, two groups of genes showed increasing regulation with time (green clusters). A similar regulation pattern was found in all members of the blue cluster. However, this was not as pronounced as in the green cluster. (B) A group of four genes was increasingly down-regulated with time (red cluster). This pattern was also found in a larger cluster (orange); therefore, the maximal regulation of these genes was less pronounced.

regulation with time. The first cluster (dark green) included *INSIG1*, *NOX 4* and *GPC4*. The second cluster (light green) included *ADAM19*, *VIM*, *HMGCS1*, *SCG5* and *FN1*. An increasing up-regulation with time was also found in an additional 29 probe sets (blue cluster). However, this was not as pronounced as in the other two clusters. A group of genes – *SERPINB3*, *KRT13* and *AQP3* (red cluster) – was increasingly down-regulated with time. Again, this pattern was found in a larger cluster (24 probe sets), but the maximum regulation of these genes was weaker (yellow cluster).

GO-analysis

GO-analysis was performed to identify known specific pathways regulated by treatment with EMD in epithelial cells. Hypergeometric testing was used to determine over-represented GO-terms attributed to the regulated genes compared with the total number of genes included in the microarray analysis. Over-represented terms of the category 'biological process' (Table 2) were distributed in various pathways. Biological processes with only one regulated gene were excluded, except for those in which only a single gene of the related process was probed. The individual highest gene distribution was seen in the category of 'developmental process' (Table 2) (GO:0032502, 12 regulated genes, $p = 0.027$), which includes, amongst others, the biological processes regulation of cell size (GO:0008361, three regulated genes, $p = 0.014$), cell growth (GO:0016049, three regulated genes, $p = 0.014$) and regulation of cell growth (GO:0001558, three regulated genes, $p = 0.007$). The second category with over-represented genes was locomotion (GO:0040011, three regulated genes, $p = 0.043$), including the processes locomotory behaviour (GO:0007626, three regulated genes, $p = 0.046$) and cell motility (GO:0048870, three regulated genes, $p = 0.043$). Other regulated pathways were anion transport (GO:0006820, three regulated genes, $p = 0.018$) and proteolysis (GO:0006508, five regulated genes, $p = 0.046$), but nodes with over-represented genes of these pathways were not at the same level of the GO-tree as the other two pathways. The same statistical algorithm was applied to the GO-terms of the category cellular component. This analysis suggested a strong involvement of genes that are involved in extracellular matrix metabolism (GO: 0031012, $p < 0.001$), and in sheet-forming (GO:0030935, $p < 0.001$) and in fibrillar collagen (GO: 0005583, $p = 0.047$) metabolism.

Table 2. Gene ontology (GO) analysis

Biological process		*p*-value	Regulated genes	Genes on array
Developmental process	GO:0032502	0.027	12	1586
Anatomical structure morphogenesis	GO:0009653	0.036	9	1090
Cell morphogenesis	GO:0000902	0.033	3	166
Regulation of developmental process	GO:0050793	0.027	3	154
Sensory organ development	GO:0007423	0.004	1	1
Growth	GO:0040007	0.025	3	149
Regulation of cell size	GO:0008361	0.014	3	120
Cell growth	GO:0016049	0.014	3	120
Regulation of cell growth	GO:0001558	0.007	3	92
Regulation of growth	GO:0040008	0.009	3	101
Cell adhesion	GO:0007155	0.001	8	514
Locomotion	GO:0040011	0.043	3	185
Cell motility	GO:0048870	0.043	3	185
Locomotory behaviour	GO:0007626	0.046	3	190
Anion transport	GO:0006820	0.018	3	132
Inorganic anion transport	GO:0015698	0.011	3	110
Phosphate transport	GO:0006817	0.002	3	63
Proteolysis	GO:0006508	0.046	5	468
Cellular protein catabolism	GO:0044257	0.046	5	468
Steroid metabolic process	GO:0008202	0.002	4	123
Activation of MAPKK activity	GO:0000186	0.004	1	1

Absolute frequencies of biological process terms of the GO-trees over-represented after stimulation of HSC-2 cells with EMD. The frequency of occurrence of related genes was summed up and compared with the overall chance that they would be found to be regulated on this microarray. Hypergeometric *p*-values for over-representation of the selected genes to all GO-terms in the induced GO graph were calculated. The biological processes of one tree were arranged together.
MAPKK, mitogen-activated protein kinase kinase.

In vitro wound healing, cell growth and cell cycle analyses

In order to measure the antimigratory effects of EMD on epithelial (HSC-2) cells, HSC-2 cells were tested using the scratch assay. After 14 h, control cells showed complete closure of the scratch. *In vitro* wound healing was clearly inhibited in cells treated with 100 μg/mL of EMD + 2% FCS for 14 h (Fig. 3). EMD-treated cells achieved complete closure of the scratch after 20 h (data not shown). The MTT assay revealed that treatment with 100 μg/mL of EMD for 20, 72 or 120 h significantly ($p < 0.05$; $p < 0.01$; $p < 0.05$) inhibited the proliferation of HSC-2 cells (Fig. 4). According to cell cycle analysis, there was no difference between control cells and those treated with EMD for 2 or 20 h (data not shown). In contrast, treatment with 100 μg/mL of EMD for 72 or 120 h induced significant arrest in G1 (Fig. 5).

Discussion

In clinical praxis, EMD seems to have a paradoxical effect on epithelial cells. On the one hand, it has a desirable inhibitory effect on epithelial downgrowth alongside the dental root during the early regenerative stages following surgery (9); on the other hand, however, accelerated epithelial soft tissue wound healing was observed upon the intrasurgical application of EMD (10). In order to accumulate more consolidated knowledge regarding the effect of EMD on

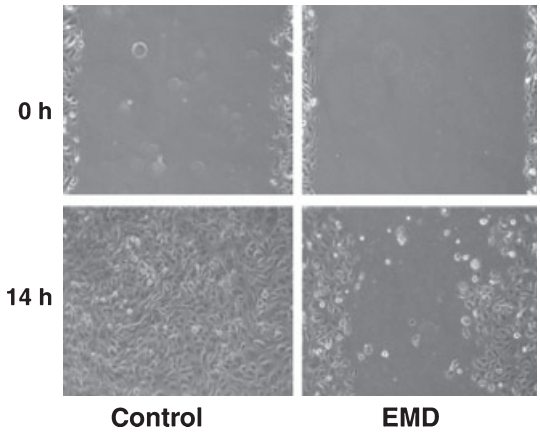

Fig. 3. Effect of EMD on the *in vitro* wound healing of HSC-2 cells. Cells were scratched with a plastic pipette tip through the confluent monolayer of HSC-2 cells. Cultures were incubated for 14 h at 37°C in the presence of 0 (Control) or 100 μg/mL of EMD in Dulbecco's modified Eagle's minimal essential medium (DMEM) containing 2% fetal calf serum (FCS).

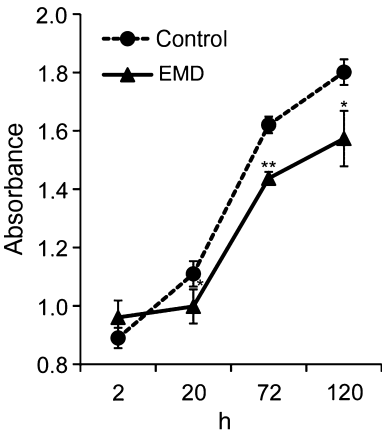

Fig. 4. Effect of 100 μg/mL of EMD on HSC-2 cell growth. After 20, 72 and 120 h of treatment, EMD-treated cells showed significantly reduced proliferation rates vs. control cells. $*p < 0.05$, $**p < 0.01$.

epithelial cells, we analyzed the changes in gene expression following EMD treatment and generated an expression profile of EMD-regulated genes in HSC-2 cells. Genome-wide transcriptome analysis is a powerful screening method for studying the molecular basis of interactions. However, the amount of tissue obtained from clinical experiments, and the complexity of these tissue samples, limit the application potential of this technique. Therefore, a human squamous carcinoma cell line was used in this study. Within the limitations of microarray technology (the presence of an appropriate probe set on the array), a set of regulated genes, possibly responsible for the effect of EMD treatment on epithelial cells, could successfully be identified. To our knowledge, this is the first expression profile of epithelial cells at different time-points (2, 20 or 120 h) of EMD treatment. A single replicate per time-point was performed for microarray analysis. However, gene-expression profiles were confirmed using an independent technique, namely real-time RT-PCR. Thus, these experiments represented independent biological repeats of the experiment. Real-time RT-PCR was performed for 43 genes in control and EMD-treated HSC-2 cells in three independent experiments. The positive correlation of 32 regulated genes between microarray and quantitative real-time RT-PCR results ($R > 0.6$) strengthened the validity of our primary data acquired by the Affymetrix gene analyses. The overall quantitative correlation between Affymetrix and real-time PCR data was only partial. Nevertheless, this was not a surprising finding as it is known that these two techniques display different sensitivities. The problems associated with analyzing expression data from a large number of genes lead to the development of alternative statistic approaches and tools (13). Cluster analysis became a popular tool for the analysis of expression array data (13). Using hierarchical clustering we identified five clusters with similar gene-expression patterns (Fig. 2). Pathway analysis identified two clusters of mainly transforming growth factor-1 (*TGF*β1) up-regulated genes, as determined by literature research. Although TGF-β1 has not been identified in EMD (5,14), many recent publications reported increased endogenous production of TGF-β1 in different cell types after EMD stimulation (4,15–18). In our data set, 20 out of the 43 EMD-regulated genes have been reported to be TGF-β1-dependent in different epithelial cell types (Table 3). Considering the possibility that the endogenous production of TGF-β1 is a result of epithelial-to-mesenchymal transition, we decided to search our data for a set of genes associated with this process. To our surprise, eight of the EMD-regulated genes – *CLDN1* (19), *CTGF* (20,21), *FN1* (22), *THBS1* (23), *TPM1* (24,25), *VIM* (21), *SRPX* (26) and *WNT5b* (27) – have previously been reported to be associated with epithelial-to-mesenchymal transition. As EMD is a product of the developing tooth root, one might hypothesize that reduced epithelial repopulation of the tooth root after periodontal surgery is the result of cell conversion from an epithelial to a mesenchymal phenotype (which is a normal process of embryonic development) rather than reduced epithelial down-growth. This hypothesis was supported by the GO-analysis identifying the individual highest gene distribution in the developmental pathways. This is not surprising, as EMD contains various amelogenins involved in the formation of periodontal attachment during tooth development (5,6). Nevertheless, GO analysis should be interpreted with caution because of the low number of probe sets. The processes of cell growth and regulation were over-represented among the developmental pathways. Therefore, a cell growth assay was performed to further investigate the effect of EMD on HSC-2 cells. Our cell-proliferation data confirmed the results of previous studies by Kawase *et al.* (8,28,29), that EMD had an antiproliferative effect on

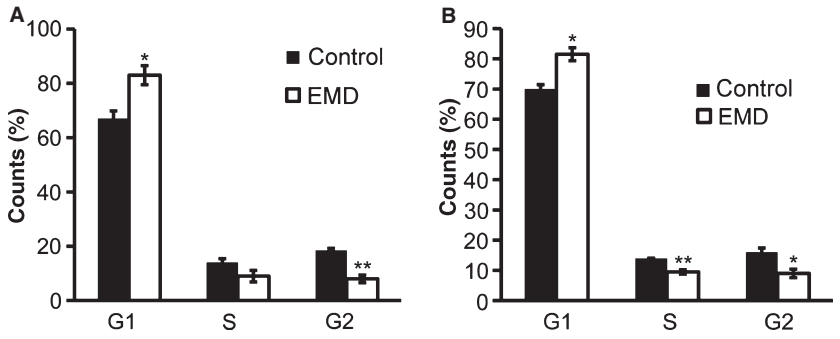

Fig. 5. Effect of EMD on cell cycle distribution in HSC-2 cells. HSC-2 cells were incubated with 100 μg/mL of EMD for 2, 20 (data not shown), 72 (A) or 120 h (B) and then stained with propidium iodide. Data represent the percentage of total cells (measured by flow cytometry) in G1, S and G2 phases of the cell cycle at each time-point. Average values ± standard deviation (SD) of three replicate experiments are shown. *$p < 0.05$, **$p < 0.01$.

Table 3. Transforming growth factor-β1 (TGF-β1)-regulated genes (according to previously published data)

Affymetrix probeset ID	Gene symbol	Regulation microarray	Regulation by TGF-β1	References
209765_at	*ADAM19*	Up	Up	(30)
39248_at, 39249_at	*AQP3*	Down	Up	(31)
218182_s_at, 222549_at	*CLDN1*	Down	Down	(30)
211981_at	*COL4A1*	Up	Up	(30,31)
212488_at	*COL5A1*	Up	Up	(32)
209101_at	*CTGF*	Up	Up	(32)
210495_x_at, 211719_x_at, 212464_s_at, 216442_x_at	*FN1*	Up	Up	(31)
210095_s_at, 212143_s_at	*IGFBP3*	Down	Down	(33)
208083_s_at	*ITGB6*	Up	Up	(30)
207935_s_at	*KRT13*	Down	Up	(31)
219909_at	*MMP28*	Up	Up	(34)
202149_at	*NEDD9*	Up	Up	(30)
233609_at, 233770_at	*PTPRK*	Up	Up	(35)
203889_at	*SCG5*	Up	Up	(36)
201416_at, 201417_at, 213668_s_at	*SOX4*	Up	Up	(30)
201107_s_at, 235086_at	*THBS1*	Up	Up	(31)
217875_s_at, 222449_at, 222450_at, 237166_at	*TMEPAI*	Up	Up	(30,31)
206116_s_at, 206117_at, 210986_s_at	*TPM1*	Up	Up	(25)
209118_s_at	*TUBA3*	Up	Up	(31)
201426_s_at	*VIM*	Up	Up	(31)

Down, down-regulated; Up, up-regulated.

the HSC-2 epithelial cell line. The antiproliferative effect was further confirmed by cell cycle analyses. In accordance with the studies performed by Kawase *et al.* (8,29), EMD induced cell cycle arrest after 72 and 120 h. In biological process GO-analysis, the pathway of locomotion showed three nodes with significantly over-represented genes. Therefore, an *in vitro* wound-healing assay was performed to investigate the effect of EMD on the migration of HSC-2 cells. EMD had an inhibitory effect on *in vitro* wound healing. *In vitro* wound-healing assays are often defined as migration assays, but *in vitro* wound healing involves several steps: spreading of the cells, migration and proliferation. Because of the very low levels of FCS, as described by Liang *et al.* (12), the proliferation rate in our *in vitro* wound-healing assays was reduced. Additionally, when studying proliferation assays of HSC-2 cells, we observed that cell division started only after 20 h, but that the closure of the scratch in our *in vitro* wound-healing assays had already been accomplished after 14 h. Nevertheless, adhesion and spreading of the cells might have a considerable contribution to these findings.

Further studies focusing on the effects of EMD during epithelial wound healing would be necessary to investigate the possible involvement of the TGF-β-regulated pathway upon EMD treatment and also to define the bioactive factors that cause the desirable inhibition of epithelial downgrowth alongside the root without epithelial wound-closure impairment.

Conclusion

Our study provides the first validated comprehensive gene-expression profile of EMD-treated human squamous epithelial cells. This profile may serve as a foundation to gain new insights into the mechanism of epithelial wound healing upon periodontal regeneration following EMD treatment and may, in the longer term, therefore also open up new opportunities for modified treatments.

Acknowledgements

This study was supported by a grant from the ITI Foundation (Grant Project Number AP00129OFF). The authors would like to thank Univ.-Doz. Dr Xiaohui Rausch-Fan for providing us with the HSC-2 cell line, as well as Straumann (Basel, Switzerland) for supplying us with EMD. Special thanks to Karin Schluifer and Quynh Nguyen Phuong for technical assistance, as well as to Katherin Patsch, MSc, for language assistance.

Supporting information

Additional Supporting Information may be found in the online version of this article:

Table S1 Regulation-values of commonly regulated genes.

Please note: Wiley-Blackwell are not responsible for the content or functionality of any supporting materials

supplied by the authors. Any queries (other than missing material) should be directed to the corresponding author for the article.

References

1. Heijl L. Periodontal regeneration with enamel matrix derivative in one human experimental defect. A case report. *J Clin Periodontol* 1997;**24:**693–696.
2. Mellonig JT. Enamel matrix derivative for periodontal reconstructive surgery: technique and clinical and histologic case report. *Int J Periodontics Restorative Dent* 1999;**19:**8–19.
3. Sculean A, Chiantella GC, Windisch P, Donos N. Clinical and histologic evaluation of human intrabony defects treated with enamel matrix derivative (Emdogain). *Int J Periodontics Restorative Dent* 2000;**20:**375–381.
4. Lyngstaadas SP, Lundberg E, Ekdahl H, Andersson C, Gestrelius S. Autocrine growth factors in human periodontal ligament cells cultured on enamel matrix derivative. *J Clin Periodontol* 2001;**28:** 181–188.
5. Saito K, Konishi I, Nishiguchi M, Hoshino T, Fujiwara T. Amelogenin binds both heparan sulfate and bone morphogenetic protein 2 and pharmacologically supresses the effect of noggin. *Bone* 2008;**43:**371–376.
6. Veis A. Ameolgenin gene splice products: potential signaling molecules. *Cell Mol Life Sci* 2003;**60:**38–55.
7. Rodrigues TL, Marchesan JT, Coletta RD *et al*. Effects of enamel matrix derivative and transforming growth factor-beta1 on human periodontal ligament fibroblasts. *J Clin Periodontol* 2007;**34:**514–522.
8. Kawase T, Okuda K, Yoshie H, Burns DM. Cytostatic action of enamel matrix derivative (EMDOGAIN) on human oral squamous cell carcinoma-derived SCC25 epithelial cells. *J Periodontal Res* 2000;**35:** 291–300.
9. Hammarström L. Enamel matrix, cementum development and regeneration. *J Clin Periodontol* 1997;**24:**658–668.
10. Sanz M, Tonetti MS, Zabalegui I *et al*. Treatment of intrabony defects with enamel matrix proteins or barrier membranes: results from a multicenter practice-based clinical trial. *J Periodontol* 2004; **75:**726–733.
11. Gentleman RC, Carey VJ, Bates DM *et al*. Bioconductor: open software development for computational biology and bioinformatics. *J Genome Biol* 2004;**5:**R80.
12. Liang CC, Park AY, Guan JL. In vitro scratch assay: a convenient and inexpensive method for analysis of cell migration in vitro. *Nat Protoc* 2007;**2:**329–333.
13. Estler M, Boskovic G, Denvir J, Miles S, Primerano DA, Niles RM. Global analysis of gene expression changes during retinoic acid-induced growth arrest and differentiation of melanoma: comparison to differentially expressed genes in melanocytes vs melanoma. *BMC Genomics* 2008;**9:**478–489.
14. Gestrelius S, Andersson C, Johansson AC *et al*. Formulation of enamel matrix derivative for surface coating. Kinetics and cell colonization. *J Clin Periodontol* 1997;**24:**678–684.
15. Okubo K, Kobayashi M, Takiguchi T *et al*. Participation of endogenous IGF-I and TGF-beta 1 with enamel matrix derivative-stimulated cell growth in human periodontal ligament cells. *J Periodontal Res* 2003;**38:**1–9.
16. Lee AZ, Jiang J, He J, Safavi KE, Spangberg LS, Zhu Q. Stimulation of cytokines in osteoblasts cultured on enamel matrix derivative. *Oral Surg Oral Med Oral Pathol Oral Radiol Endod* 2008;**106:**133–138.
17. Hama H, Azuma H, Seto H, Kido J, Nagata T. Inhibitory effect of enamel matrix derivative on osteoblastic differentiation of rat calvaria cells in culture. *J Periodontal Res* 2008;**43:**179–185.
18. Grayson RE, Yamakoshi Y, Wood EJ, Agren MS. The effect of the amelogenin fraction of enamel matrix proteins on fibroblast-mediated collagen matrix reorganization. *Biomaterials* 2006;**27:**2926–2933.
19. Kojima T, Takano K, Yamamoto T *et al*. Transforming growth factor-beta induces epithelial to mesenchymal transition by down-regulation of claudin-1 expression and the fence function in adult rat hepatocytes. *Liver Int* 2008;**28:**534–545.
20. Gressner OA, Gressner AM. Connective tissue growth factor: a fibrogenic master switch in fibrotic liver diseases. *Liver Int* 2008;**28:**1065–1079.
21. Liu BC, Zhang JD, Zhang XL, Wu GQ, Li MX. Role of connective tissue growth factor (CTGF) module 4 in regulating epithelial mesenchymal transition (EMT) in HK-2 cells. *Clin Chim Acta* 2006;**373:** 144–150.
22. Tiezzi DG, Fernandez SV, Russo J. Epithelial mesenchymal transition during the neoplastic transformation of human breast epithelial cells by estrogen. *Int J Oncol* 2007;**31:**823–827.
23. Hu Y, Jian X, Peng J, Jiang X, Li N, Zhou S. Gene expression profiling of oral submucous fibrosis using oligonucleotide microarray. *Oncol Rep* 2008;**20:**287–294.
24. Safina AF, Varga AE, Bianchi A *et al*. Ras alters epithelial-mesenchymal transition in response to TGFbeta by reducing actin fibers and cell-matrix adhesion. *Cell Cycle* 2009;**8:**284–298.
25. Zheng Q, Safina A, Bakin AV. Role of high-molecular weight tropomyosins in TGF-b-mediated control of cell motility. *Int J Cancer* 2008;**122:**78–90.
26. Feng MY, Wang K, Shi QT, Yu XW, Geng JS. Gene expression profiling in TWIST-depleted gastric cancer cells. *Anat Rec (Hoboken)* 2009;**292:**262–270.
27. Heller RS, Dichmann DS, Jensen J *et al*. Expression patterns of Wnts, Frizzleds, sFRPs, and misexpression in transgenic mice suggesting a role for Wnts in pancreas and foregut pattern formation. *Dev Dyn* 2002;**225:**260–270.
28. Kawase T, Okuda K, Momose M, Kato Y, Yoshie H, Burns DM. Enamel matrix derivative (EMDOGAIN) rapidly stimulates phosphorylation of the MAP kinase family and nuclear accumulation of smad2 in both oral epithelial and fibroblastic human cells. *J Periodontal Res* 2001;**36:** 367–376.
29. Kawase T, Okuda K, Yoshie H, Burns DM. Anti-TGF-beta antibody blocks enamel matrix derivative-induced upregulation of p21WAF1/cip1 and prevents its inhibition of human oral epithelial cell proliferation. *J Periodontal Res* 2002;**37:**255–262.
30. Levy L, Hill CS. Smad4 dependency defines two classes of transforming growth factor {beta} (TGF-{beta}) target genes and distinguishes TGF-{beta}-induced epithelial-mesenchymal transition from its antiproliferative and migratory responses. *Mol Cell Biol* 2005;**25:**8108–8125.
31. Ranganathan P, Agrawal A, Bhushan R *et al*. Expression profiling of genes regulated by TGF-beta: differential regulation in normal and tumour cells. *BMC Genomics* 2007;**11:**98–116.
32. Keating DT, Sadlier DM, Patricelli A *et al*. Microarray identifies ADAM family members as key responders to TGF-beta 1 in epithelial cells. *Respir Res* 2006;**7:** 114–129.
33. Edmondson SR, Murashita MM, Russo VC, Wraight CJ, Werther GA. Expression of insulin-like growth factor binding protein-3 (IGFBP-3) in human keratinocytes is regulated by EGF and TGFB-1. *J Cell Physiol* 1999;**179:**201–207.
34. Saarialho-Keere U, Kerkela E, Jahkola T, Suomela S, Keski-Oja J, Lohi J. Epilysin (MMP-28) expression is associated with cell proliferation during epithelial repair. *J Invest Dermatol* 2002;**119:**1–21.
35. Wang SE, Wu FY, Shin I, Qu S, Arteaga CL. Transforming growth factor (TGF)-smad target gene protein tyrosine phosphatase receptor type kappa is required for TGF- Function. *Mol Cell Biol* 2005; **11:**4703–4715.
36. Cheng CF, Fan J, Bandyopahdhay B *et al*. Profiling motility signal-specific genes in primary human keratinocytes. *J Invest Dermatol* 2008;**128:**1981–1990.